(1968).
[12]M. C. Montmory and R. Newnham, Solid State Commun. 6, 1359 (1968).
[13]M. C. Montmory, M. Belakhovsky, R. Chevalier, and R. Newnham, Solid State Commun. 6, 317 (1968).
[14]H. J. Guggenheim, M. T. Hutchings, and B. D. Rainford, J. Appl. Phys. 39, 1120 (1968).
[15]J. W. Stout and S. A. Reed, J. Am. Chem. Soc. 76, 5279 (1954).
[16]A. Okazaki, K. C. Turberfield, and R. W. H. Stevenson, Phys. Letters 8, 9 (1964).
[17]M. Butler, V. Jaccarino, N. Kaplan, and H. J. Guggenheim, Phys. Rev. B 1, 3085 (1970).
[18]G. K. Wertheim, H. J. Guggenheim, M. Butler, and V. Jaccarino, Phys. Rev. 178, 804 (1969).
[19]F. Keffer, Phys. Rev. 87, 608 (1952).
[20]M. E. Lines, Phys. Rev. 156, 543 (1967).
[21]See, e. g., P. W. Anderson, in *Magnetism*, edited by G. T. Rado and H. Suhl (Academic, New York, 1963), Vol. I.
[22]O. Berkooz, M. Melamud, and S. Shtrikman, Solid State Commun. 6, 185 (1968).
[23]I. Bransky, N. M. Tallan, and A. Z. Hed, J. Appl. Phys. 41, 1787 (1970).

PHYSICAL REVIEW B VOLUME 6, NUMBER 5 1 SEPTEMBER 1972

Magnon Heat Conduction and Magnon Scattering Processes in Fe-Ni Alloys*

W. B. Yelon† and L. Berger
Physics Department, Carnegie-Mellon University, Pittsburgh, Pennsylvania 15213
(Received 3 January 1972; revised manuscript received 19 April 1972)

The thermal and electrical conductivities of 70-wt%-Ni–30-wt%-Fe, 81-wt%-Ni–19-wt%-Fe, and 67-wt%-Ni–33-wt%-Cu have been measured between 1.5 and 4.5 K, in external fields up to 6 T. Both nickel-iron alloys show a small magnon contribution κ_m to the thermal conduction, equal to about 3% of the total conductivity at 4 K. In 70-wt%-Ni–30-wt%-Fe $\kappa_m \propto T^{1.9}$ is found. Using a simple kinetic-theory model, the magnon lifetime τ_m is derived equal to 1.7×10^{-10} sec at 4 K and varying as $T^{-0.6}$. This implies $\tau_m \propto \omega^{-0.6}$. In the zero-magnetostriction alloy 81-wt%-Ni–19-wt%-Fe, $\kappa_m \propto T^{1.5}$ and $\tau_m \propto T^{-1} \propto \omega^{-1}$ is found to hold. Our lifetime values agree with those derived from magnetic resonance linewidths. The nickel-copper alloy shows no magnon heat transport, implying a magnon lifetime of less than 2×10^{-11} sec at 3.55 K. Shorter magnon lifetime in Ni-Cu than in Ni-Fe may reflect faster magnon-electron relaxation, corresponding to increased smearing of the electron momentum gap by alloy disorder. The latter correlates, in turn, with larger electrical resistivity and smaller magnetization.

I. INTRODUCTION

Magnons can be expected to carry a sizable heat current in any ferromagnetic or antiferromagnetic material if the magnon lifetime is long enough. This magnon conduction has been observed in insulators, both ferro-[1,2] and antiferromagnetic.[3,4] There is also evidence of magnon conduction in ferromagnetic rare earths,[5] but there have been no similar reports for transition metals. This is because the separation of the magnon contribution from that of the electrons and phonons has been a very difficult problem. However, in concentrated alloys we expect that the magnon contribution may be seen because of its distinctive field dependence, the electron and phonon contributions being essentially field independent above saturation.

This work is an investigation of three ferromagnetic alloys, 70-wt%-Ni–30-wt%-Fe, 81-wt%-Ni–19-wt%-Fe, and 67-wt%-Ni–33-wt%-Cu. The thermal conductivity was measured in the temperature range 1.5–4.5 K, in magnetic fields up to 6 T. A preliminary report on this piece of research has already been published.[6]

II. ELECTRON AND PHONON THERMAL CONDUCTION

In our concentrated alloys at $T < 4$ K, electrons are scattered mostly by impurities. For example, we have checked that the electrical resistivity ρ of 81-wt%-Ni–19-wt%-Fe is constant to better than ±0.2% between 1.5 and 4.2 K, in a constant field of 0.715 T. Since this scattering is elastic, the Wiedemann-Franz law is expected to hold,[7] even in a magnetic field:

$$\kappa_e = \frac{\pi^2 k_B^2}{3e^2\rho} T ,$$

where κ_e is the electronic thermal conductivity and k_B the Boltzmann constant. Thus we can calculate κ_e from the measured ρ value. In concentrated alloys, ρ and κ_e are actually found to change very little above ferromagnetic saturation. This happens because $\omega_c\tau \ll 1$, where ω_c is the electron cyclotron frequency.

These alloys show a ferromagnetic anisotropy of the resistivity; that is, their electrical and thermal resistivities change considerably from zero applied field to technical saturation.[8] In

parallel fields the resistivity increases; in perpendicular fields it decreases. Because this change is large in the two Ni-Fe alloys, and because the demagnetized state at zero applied field is not very reproducible, we do not attempt to use the Wiedemann-Franz law in the region from zero applied field to saturation. The most important data are obtained above saturation.

Pippard developed a theory of ultrasonic attenuation in alloys,[9] taking into account the effect of finite electron mean free path. This was applied to the phonon-thermal-conductivity problem by Zimmerman[10] and by Lindenfeld and Pennebaker.[11] The success of this theory in explaining phonon-thermal-conductivity data implies that electrons are the most important cause of phonon scattering, even in alloys. A moderate amount of phonon-impurity scattering probably exists too.

On the other hand, magnons are too few at $T < 20$ K for phonon-magnon scattering to be important in metals and alloys.

Since $\omega_c \tau \ll 1$ in these alloys, the electronic system is practically not affected by the presence of a magnetic field. As a consequence, phonon-electron scattering and, in turn, the phonon thermal conductivity are independent of magnetic field. This would not be true in the case of pure metals, where the magnetoacoustic effect exists, and for this reason they may not be suitable for studies of magnon heat transport.

III. THERMAL CONDUCTION BY MAGNONS

Douthett and Friedberg[1] developed a model for the thermal conduction by magnons in ferromagnetic insulators, using simple kinetic theory. Their model works well for yittrium-iron garnet (YIG) and reasonably well for other insulators in which the magnon-phonon interaction is not too strong. For our work we use a similar model.

The thermal conductivity of a magnon gas is

$$\kappa_m = \tfrac{1}{3} \sum c v \Lambda_m = \tfrac{1}{3} \sum c v^2 \tau_m ,$$

where c is the specific heat, v is the velocity, Λ_m is the mean free path, and τ_m is the relaxation time of a magnon mode. Douthett and Friedberg assumed, correctly, that for their good single-crystal and large-grained polycrystal insulators the magnons are scattered by the grain boundaries with a constant mean free path; hence they used the first formalism. We have used the relaxation-time formalism since most discussions of magnon scattering in metals consider the relaxation time rather than the mean free path.

The sum above may be written as an integral:

$$\kappa_m = \tfrac{1}{3} \int \tau_m c(q) v^2 \frac{dN}{dq} dq .$$

This is evaluated by making the following substitutions:

$$E(q) = Dq^2 + g\mu_B B_{eff} = \hbar\omega , \quad v(q) = \frac{d\omega}{dq} = 2Dq/\hbar ,$$

$$\frac{dN}{dq} = q^2/2\pi^2 ,$$

$$c(q) = \frac{\partial}{\partial T}[U(q)] = \frac{\partial}{\partial T} \frac{E(q)}{\exp(E/k_B T) - 1} ,$$

$$x = Dq^2/k_B T, \qquad y = g\mu_B B_{eff}/k_B T .$$

We arrive at the final form:

$$\kappa_m = \frac{k_B^{7/2} T^{5/2}}{3\hbar^2 D^{1/2} \pi^2} \int \tau_m \frac{(x+y)^2 x^{3/2} e^{x+y}}{(e^{x+y}-1)^2} dx . \qquad (1)$$

We now can make either of two plausible assumptions about the behavior of τ_m in order to evaluate this expression.

The simpler assumption ("average-lifetime model") is that we take τ_m as frequency independent or as some temperature-dependent average $\bar{\tau}_m$ over all the magnons contributing to the transport. In that case we take $\bar{\tau}_m$ out of the integral:

$$J(y) = \int_0^\infty \frac{(x+y)^2 x^{3/2} e^{x+y}}{(e^{x+y}-1)^2} dx ,$$

$$\kappa_m = \frac{k_B^{7/2} T^{5/2}}{3\pi^2 \hbar^2 D^{1/2}} \bar{\tau}_m J(y) , \qquad (2)$$

where the upper limit can be approximated as $+\infty$ if T is sufficiently low, and where $J(0) = \Gamma(\frac{9}{2}) \zeta(\frac{7}{2}) = 13.1$.

If the effective field B_{eff} vanishes, then $y = 0$ and the temperature dependence of the magnon thermal conduction is $T^{5/2}$ (times the dependence of the lifetime, if any), in contrast to the T^2 dependence predicted by the Douthett-Friedberg model. What is particularly striking is the weak dependence on the exchange stiffness D, which is such that the smaller the stiffness the larger the thermal conduction (since magnons are more easily excited in this case).

It is interesting to look more closely at the expression inside the integral in Eq. (2) which represents the contribution by frequency to the magnon conduction. This is plotted in Fig. 1 for $B_{eff} = 0$, and shows a peak at $\hbar\omega = 3.2 k_B T$. It appears that most of the conduction is from a relatively narrow band of frequencies around that peak. We therefore associate the average lifetime $\bar{\tau}_m$ with the average frequency $\bar{\omega} = 3.2 k_B T/\hbar$. As we have assumed that the lifetime is not strongly frequency dependent, this should be a reasonable procedure.

The magnetic field dependence of the integral $J(y)$ of Eq. (2) is shown in Fig. 2. This represents also the percentage of the $B_{eff} = 0$ magnon conduction present at any given field and temperature.

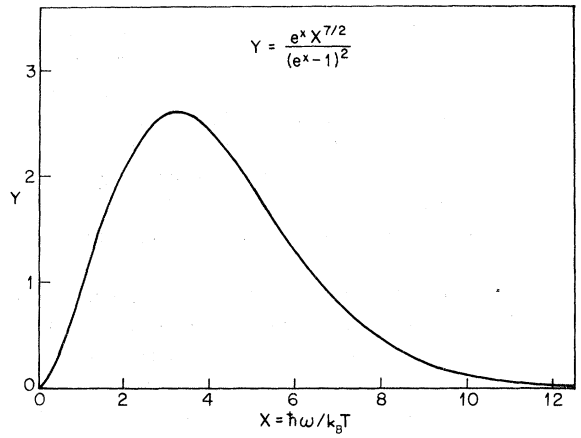

FIG. 1. Relative contribution Y of magnons of various frequencies to the thermal conductivity, for the average lifetime model, at $B_{eff}=0$.

Of course, this formalism is meaningful only if the relaxation time is well defined, e. g., if the magnons are created or annihilated by the electrons in one-magnon processes, or undergo large-angle scattering on impurities.

A different assumption, which is actually a special case of the first one, is that $\tau_m = b\omega^{-1/2}$. This frequency dependence is the one predicted from the theory of magnon scattering by conduction electrons via the s-d exchange interaction,[12,13] assuming that the so-called "momentum gap" may be neglected. Then we obtain from Eq. (1)

$$\kappa_m = \frac{k_B^3 T^2 b}{3\pi^2 \hbar^{3/2} D^{1/2}} \int_0^\infty \frac{(x+y)^{3/2} x^{3/2} e^{x+y}}{(e^{x+y}-1)^2}\, dx \,. \tag{3}$$

Considering the case $B_{eff}=0$ (that is $y=0$) the magnon thermal conductivity is proportional to T^2. Also, in that case the integrand in Eq. (3) peaks at $2.6 k_B T$ rather than $3.2 k_B T$, because the shorter lifetime at higher frequencies tends to diminish somewhat the importance of the higher-energy magnons to the conduction process.

The integral of Eq. (3) and the integral $J(y)$ of Eq. (2) (Fig. 2) have very similar y dependence, but the first one tends to fall off more quickly, again because of the smaller importance of high-energy magnons.

It is interesting to note that the s-d exchange model gives the same dependence $\kappa_m \propto T^2$ as the Douthett-Friedberg boundary-scattering model. This was to be expected since the relation $\tau_m \propto \omega^{-1/2}$ implies a constant mean free path, which is the assumption Douthett and Friedberg made. Nevertheless, the scattering mechanisms are quite different, and also the lifetime values: $\approx 10^{-10}$ sec in metals vs $\approx 10^{-8}$ sec in YIG.

Either of our models includes the assumption that the lifetime for a given *frequency* magnon is independent of the external magnetic field. This sounds reasonable until one realizes that it differs from the assumption that the lifetime be a constant at given wave number, since the relation $\hbar\omega = Dq^2 + g\mu_B B_{eff}$ depends explicitly on B_{eff}. Anyway, we will see that our assumption leads to a fair agreement with the experiments.

We have carefully avoided defining B_{eff} so far, since the situation is theoretically somewhat more complicated than we have portrayed. If we take dipole-dipole interaction into account (see the Appendix) the magnon energy is actually given (to first order in M_s) by

$$E(q) = Dq^2 + g\mu_B(B_E + \tfrac{1}{2}M_s \sin^2\theta)\,, \tag{4}$$

where B_E is the external magnetic induction, M_s the saturation magnetization in mks units, and θ the angle between $\vec{M}_s$ and $\vec{q}$. If we use this dispersion relation to calculate κ_m, we obtain Eq. (2) or Eq. (3) as before (see the Appendix), provided we write

$$B_{eff} = B_E + \tfrac{7}{15}M_s \,. \tag{5}$$

IV. THERMAL-CONDUCTIVITY MEASUREMENTS

Since magnon effects are expected to be quite small, it is necessary to put unusual care into the experimental details. For example, thermometer calibrations and avoidance of heat leaks in and out of the sample must be especially thorough. We have been able to make thermal-conductivity measurements accurate, in most cases, to about $\pm 0.3\%$.

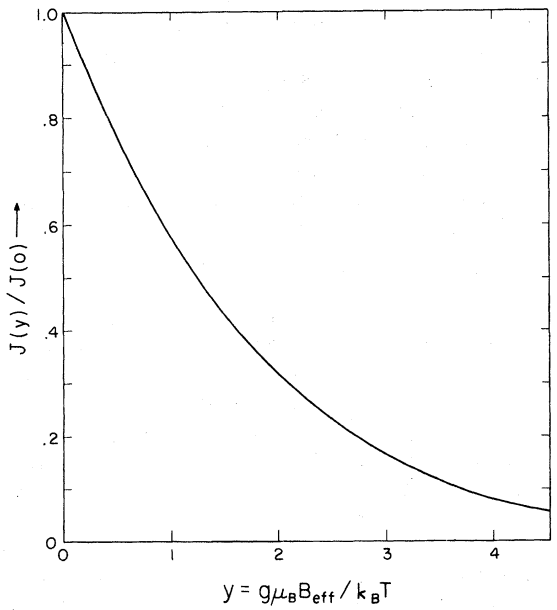

FIG. 2. Predicted magnon thermal conductivity at a field B_{eff}, normalized to the conductivity at $B_{eff}=0$.

The apparatus is of conventional design. The upper end of the cylindrical sample is thermally connected to the bath through a brass rod, inside a vacuum can ($p = 10^{-5}$ Torr). An electric heater H_1, attached at the free lower end of the sample, provides the heat current through the sample. A heater H_2 is wound around the brass rod and may be used to raise the average sample temperature. The voltage across H_1 is measured with a digital voltmeter, and so is the voltage across a standard resistor in series with H_1.

Carbon resistance thermometers R_1 and R_2 are attached at two points along the sample. Each thermometer is glued inside a hole in a copper block which is soldered to a ring of No. 20 copper wire encircling the sample. The wire can be tightened with a small screw. This gives intimate mechanical contact, together with minimum contact length along the sample.

Electrical connections to the thermometers and heaters are made through 1-in. pieces of 0.001-in.-diam manganin wire, in order to prevent heat leaks. These wires are in turn soldered to No. 36 copper leads glued together in a ribbon. The ribbon is carefully wound about 15 turns around a copper heat sink and fastened with GE-7031 varnish, in order to short circuit any heat conducted down the leads. Copper radiation baffles are soldered into the vacuum line.

The carbon resistance thermometers are placed in the arms of an ac bridge with high-gain tuned amplifier and phase-sensitive detector. Excitation voltage of bridge is typically 20 mV rms. With 1-kΩ thermometer resistance and 10-kΩ fixed arms, we can observe changes (near balance) of less than $\frac{1}{100}$ Ω. The bridge circuit[14] is such that the resistance R_1 of the first thermometer is measured directly, and also $R_1 - R_2$. This is a protection against temperature drifts.

The 100-Ω Allen-Bradley $\frac{1}{10}$-W carbon resistance thermometers are adequately described over the temperature interval 1–20 K by the modified Clement-Quinnell formula[15]:

$$1/T = a/\ln R + b + c\ln R + d(\ln R)^2 . \quad (6)$$

T is derived from the bath pressure, measured with mercury and oil manometers. Functional forms to describe the T-58 temperature scale for liquid helium were devised by Pierce.

$R_1(T)$ and $R_2(T)$ are computer fitted to Eq. (6) in such a way that $\sum(\Delta T/T)^2$ is minimized, therefore keeping the relative error $\Delta T/T$ roughly equal over the whole temperature range.

It is found that, even after correcting for the hydrostatic head of liquid helium, the experimental $R_1(T)$, $R_2(T)$ curves show a discontinuity at the λ point. This effect has been seen by other experimenters but has not always been satisfactorily dealt with. The source of this problem may be the local superheating of the bath at points in between the bubbles, above the λ point. Heat flow into the Dewar vessel creates this superheating, in turn causing the bubbles to grow. This is borne out by the observation that the discontinuity is smaller in vessels with lower boil-off rate, and is smaller when helium rather than nitrogen surrounds the inner Dewar vessel.

We experimented with several artificial corrections, but the most satisfactory one is to remove the discontinuity by adding a constant correction to the measured hydrostatic head at all pressures above the λ point. Prior to this correction, typical rms deviations from a perfect fit to Eq. (6) averaged 2–4 mK; after correction they are reduced to 0.5–1.5 mK. Moreover, when the thermal-conductivity data for different runs are compared, they agree far better after correction, despite the fact that the correction is quite different for different runs. Even after correction, systematic errors in thermometer calibration are the main factor limiting the accuracy of our thermal-conductivity measurements.

A Cartesian manostat regulates the bath temperature to about 1–2 mK. After it stabilizes, a differential oil manometer with a phototransistor sensor controls a heater to vary the helium boil-off rate.[16] Thus the temperature is held constant to ±0.1 mK at 4 K. The regulation is better than with most Sommers regulators down to 1.8 K.

The magnetic field is parallel to the heat current and is provided by a superconducting solenoid with 1% uniformity in a 1-in.-diam spherical volume. In most cases it is used in the persistent mode, to ensure field stability. Measurements are made at fixed field and variable temperature. Calibration data are taken during the same run, thereby avoiding any time-dependent effects in the thermometers.

The electrical resistivity is measured with a four-lead system, using a Leeds-and-Northrup K-3 potentiometer. Potential leads are soldered on the copper rings holding the two carbon thermometers. The sample is immersed directly in the bath. Currents up to 10 A are used, and the accuracy for the electrical resistivity is ±0.2%.

V. SAMPLE PREPARATION

The copper-nickel sample was prepared by melting, in an induction furnace, high-purity Johnson-Matthey metals, under a vacuum (prior to heating) of 6×10^{-6} Torr. After cooling, the sample was machined to a round rod and homogenized in an electric furnace at 1300 °C for 24 h, in a helium atmosphere purified by charcoal trap. The temperature was lowered to 1000 °C, the heli-

um evacuated, the sample annealed at 10^{-5} Torr for an additional $\frac{1}{2}$ h, and finally furnace cooled.

The sample was then swaged to a diameter of 0.797 cm and then annealed at 750 °C for 1 h at 6×10^{-6} Torr. The sample shows grains 0.1–0.5 mm in diam. Wet chemical analysis indicates 33.4 wt% Cu.

The nickel-iron samples were prepared in a different fashion from the Ni-Cu. Rods of J-M nickel and iron were cut into pieces of 0.3-in. length and the pieces fused together into a lump by melting each piece individually onto the preceding pieces with a levitation melter. This was done in a charcoal-trapped argon atmosphere and both samples were prepared at the same time. These rough ingots were remelted (in another levitation melter) and cast into 0.5-in.-diam molds in a helium atmosphere. During each melt there was no visible evidence of oxidation of the materials.

The 70-wt%-Ni–30-wt%-Fe alloy was swaged to $\frac{5}{16}$-in. diam and then homogenized in a flow of very pure dry hydrogen at 1200 °C for about 38 h. It was then cooled to 900 °C, the furnace was evacuated, and the sample was annealed for 2 h more to remove any dissolved hydrogen, after which it was furnace cooled. Wet analysis indicates 29.8 wt% Fe. The 81-wt%-Ni–19-wt%-Fe sample was remelted in the levitation melter to remove a large hole, then was swaged, and had the same heat treatment as the other Ni-Fe alloy. Wet analysis gives 18.9 wt% Fe. Both Ni-Fe samples have grains about 0.1–0.5 mm in diam.

VI. Ni-Cu RESULTS

The electrical resistivity at 4.2 K (at saturation) is 23.4×10^{-8} Ω m. It increases by $\Delta\rho_{\parallel}/\rho = +3\%$ from zero external field to saturation and varies by only 0.5% in the range $B_E = 0.4$–6 T above saturation, having a broad maximum at 2 T.

The thermal conductivity was measured during an early stage of development of the apparatus, and the over-all precision was not as high as for the later measurements on the Ni-Fe. The data are shown in Fig. 3 for $B_E = 0$ and $B_E = 5.9$ T, in the range 1.5–4.1 K. The thermal conductivity κ is quite small. Comparing the actual Lorenz number $L = \kappa\rho/T$ to the theoretical electronic Lorenz number $L_{th} = 2.44\times10^{-8}$ mks, we find $L/L_{th} \approx 3.3$ at 4 K, indicating that phonons or magnons conduct more heat than electrons. The calculated electronic conductivity $\kappa_e = L_{th}T/\rho$ is shown as a solid line. The magnetic field affects the thermal conductivity very little (Fig. 3). This implies a very small magnon contribution and, in turn, a very short magnon lifetime. We have performed a more detailed statistical analysis of the data in the smaller range 3.5 K–4.1 K. The standard deviation of individual datum points is about 1.4% of the

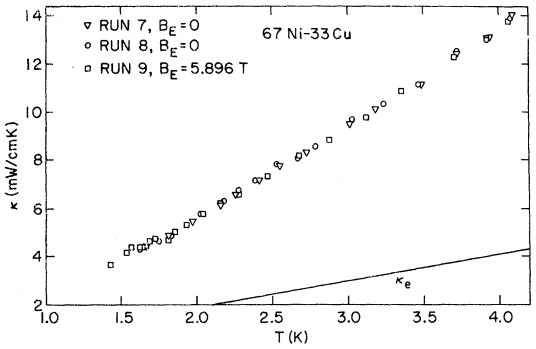

FIG. 3. Measured thermal conductivity of 67-wt%-Ni–33-wt%-Cu at $B_E = 0$ and $B_E = 5.90$ T and the calculated electronic thermal conductivity κ_e.

total κ at $B_E = 0$ and about 1.2% at $B_E = 5.90$ T. The $\Delta\rho_{\parallel}/\rho = +3\%$ field variation of electrical resistivity mentioned above is caused by the ferromagnetic anisotropy of resistivity, and implies[8] a corresponding variation $\Delta\kappa_{\parallel}/\kappa \approx -(L_{th}/L)\,\Delta\rho_{\parallel}/\rho \approx -0.9\%$ of the thermal conductivity. This systematic error has to be taken into account. Finally, averaging over all data in the interval 3.5–4.1 K, we find that the field variation of κ attributable to magnons is at most −0.9%, to 95% confidence level. Using[17] $D = 2.0\times10^{-40}$ J m^2 and Eq. (2), this will set an upper limit to the magnon lifetime of $\tau_m \lesssim 2\times10^{-11}$ sec at 3.55 K, again to 95% confidence level.

It might be expected that magnons are scattered strongly by the magnetic disturbances on the copper sites. It is well known that the nickel atoms near the copper sites have reduced magnetic moments, increasing the size of the magnetic disturbance.[18] In addition, atomic "clusters" have been observed in these alloys, or clouds of greater or lesser than average magnetization.[19] All of these factors can reduce the magnon lifetime and thus explain our negative result for Ni-Cu. However, recent Peltier-effect data[20] on the same alloy seem to show a large magnon-drag effect, suggesting that thermal magnons at 4 K are scattered more by electrons than by lattice defects or by alloy or magnetic disorder. If we accept this piece of evidence, we are forced to conclude that the short magnon lifetime in Ni-Cu reflects the existence of unusually strong electron-magnon scattering. Possible reasons for this occurrence will be discussed in Sec. VIII.

VII. Ni-Fe RESULTS

The two alloys show similar behavior for the thermal conductivity (see Figs. 4 and 5). The electrical resistivity at saturation in the longitudinal field is 4.24×10^{-8} Ω m for the 70-wt%-Ni–30-wt%-Fe, and 4.32×10^{-8} Ω m for the 81-wt%-Ni–19-wt%-Fe. It was measured in external fields up to

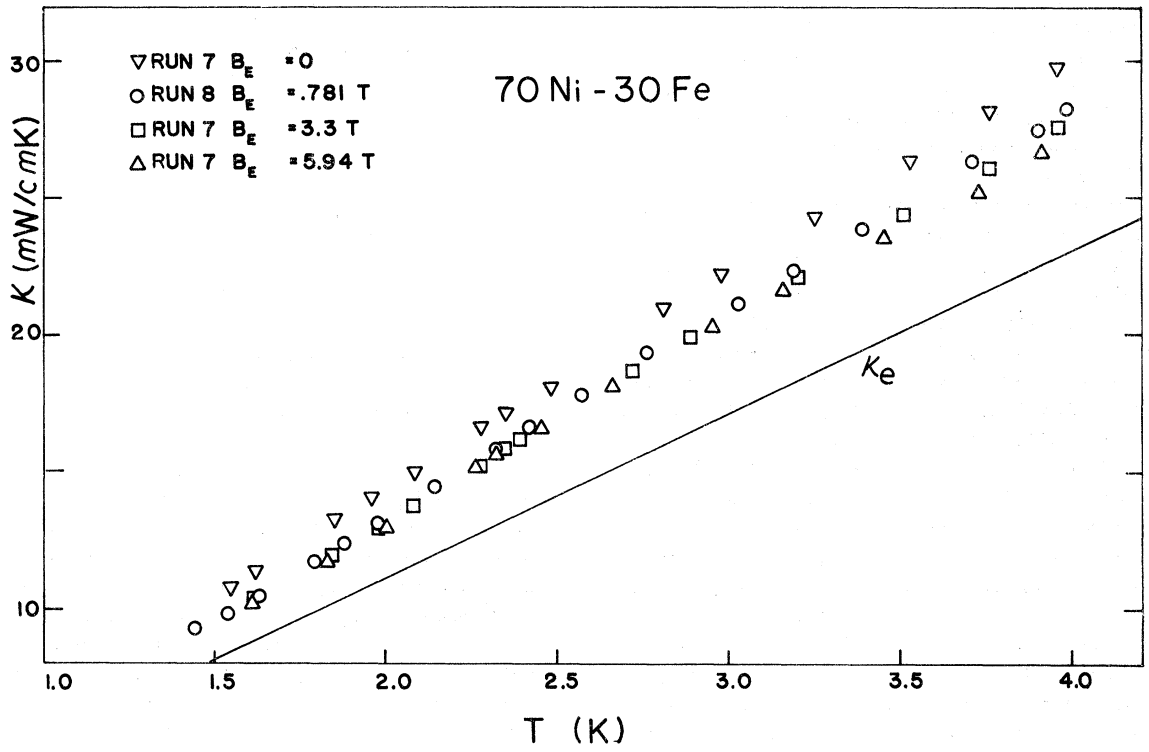

FIG. 4. Measured thermal conductivity of 70-wt%-Ni–30-wt%-Fe at $B_E = 0$ and three external fields. κ_e is the calculated electron thermal conductivity at saturation.

5.5 T. Above saturation, the 70-wt%-Ni–30-wt%-Fe shows a linear increase in resistivity of less than 0.4% while the 81-wt%-Ni–19-wt%-Fe shows no change. The 70-wt%-Ni–30-wt%-Fe has a sharp narrow peak in the resistivity just at saturation ($B_E = 0.1$ T) which probably occurs when domains start rotating. Such a peak has been observed in other permalloys.[8] The 81-wt%-Ni–19-wt%-Fe does not show any peak. The electrical resistivity of the 81-wt%-Ni–19-wt%-Fe was also measured from 4.2 down to 1.5 K and is constant to 0.2% in that range.

In Figs. 4 and 5 the calculated electronic thermal conductivity is shown along with the total measured thermal conductivity at several fields. Although the electrons are now responsible for most of the thermal conductivity, there is still a considerable contribution that is unaccounted for by just the electron conductivity. This contribution is primarily due to the phonons, as with the Ni-Cu, but the field dependence of the thermal conductivity above saturation shows that there is also a magnon contribution. Since Figs. 4 and 5 are on too small a scale to do full justice to the high accuracy of the data in a magnetic field, we show on a larger scale in Fig. 6 the change in thermal conduction as compared to $B_E = 0$, for the alloy 70-wt%-Ni–30-wt%-Fe. Through graphical data averaging and linear interpolation, the number of points shown has actually been reduced to a few, located at regular temperature intervals of half a degree.

As mentioned in Sec. II, because of the large ferromagnetic anisotropy of resistivity it is advisable to use only data obtained above ferromagnetic saturation. Table I, column 2 shows the total change $\Delta\kappa$ in the thermal conductivity between $B_E \approx 0.75$ and 5.94 T at several standard temperatures, and column 3 shows the electronic contribution $\Delta\kappa_e$ to that change calculated from the Wiedemann-Franz law. The difference between columns 2 and 3 corresponds to the change $\Delta\kappa_m$ in the magnon thermal conduction, tabulated in column 4.

From the theory of Sec. III we can calculate at any temperature the fractional change $\Delta\kappa_m/\kappa_m$ of the total magnon conductivity between two values of the field B_{eff}. For example, Eq. (2) gives

$$\frac{\Delta\kappa_m}{\kappa_m(B_{eff}=0)} = \frac{\Delta J}{J(0)} = \frac{\Delta J}{13.1}, \tag{7}$$

where ΔJ is the corresponding change of the integral $J(y)$. This is plotted in column 5. The two B_{eff} values, from Eq. (5), are $B_{eff} \approx 1.38$ and 6.57 T since[21] $M_s \approx 1.36$ T. We assume[22] $g = 2.14$.

Combining column 4 and column 5, we obtain

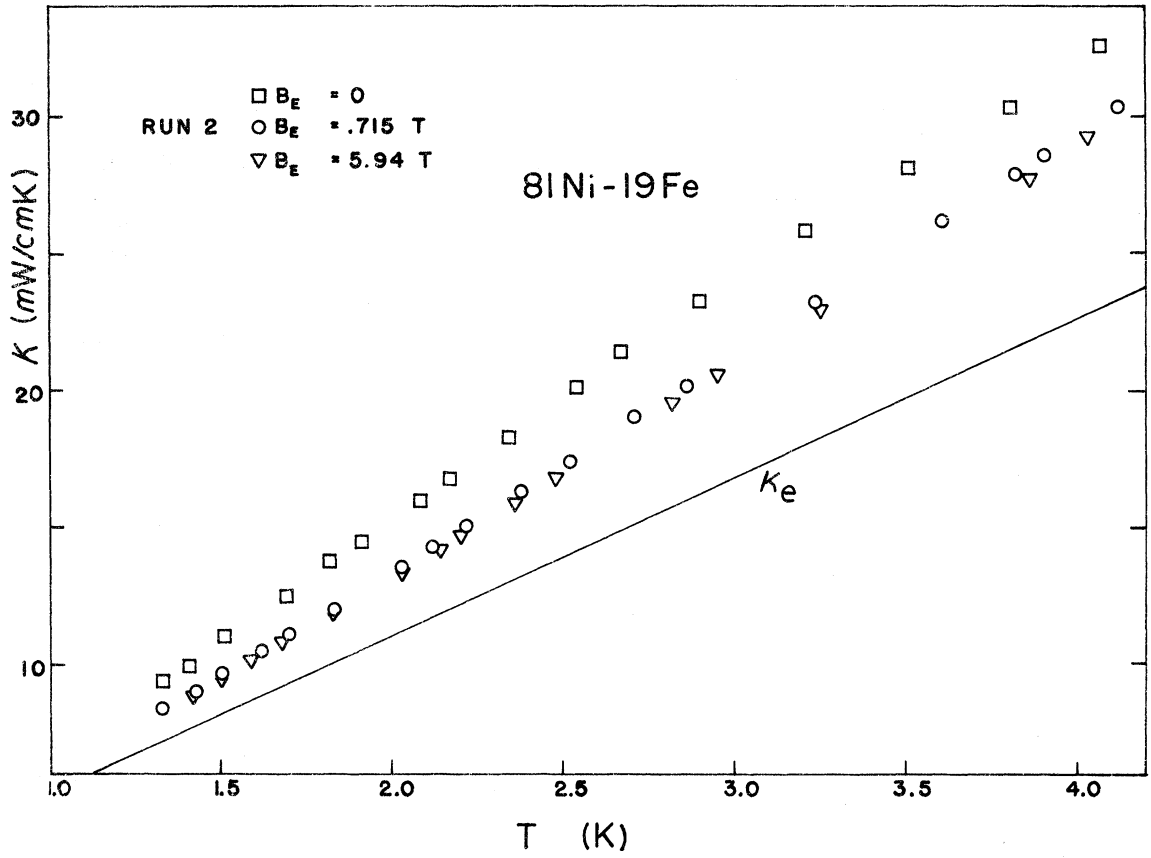

FIG. 5. Measured thermal conductivity of 81-wt%-Ni–19-wt%-Fe at $B_E = 0$, and two external fields. κ_e is the calculated electron thermal conductivity at saturation.

values of the full magnon conductivity κ_m at $B_{eff} = 0$, plotted in column 6, and in Fig. 7. Also shown in Fig. 7 is the total experimental thermal conductivity κ at $B_E = 0$. We see that magnon conduction is only about 3% of the total thermal conduction in this 70-wt%-Ni–30-wt%-Fe alloy.

The dashed curve in Fig. 6 shows the conductivity change from $B_E = 0$ to $B_E = 3.3$ T predicted from the κ_m values of column 6, using Eq. (7). It agrees very well with the data taken at that field. This is a check that Eqs. (2) and (7) are valid, and that $\bar{\tau}_m$ is roughly field independent.

The zero-field magnon conductivity κ_m of 70-wt%-Ni–30-wt%-Fe varies like $T^{1.9}$ (see Fig. 7). According to Eq. (2), this implies a magnon lifetime $\bar{\tau}_m \propto T^{-0.6}$. Values of $\bar{\tau}_m$ are plotted in column 7 of Table I. We assume[22] $D = 3.83 \times 10^{-40}$ J m^2. The average magnon frequency $\bar{f} = \bar{\omega}/2\pi$ is given in column 8, based on the relation $\bar{\omega} = 3.2 k_B T/\hbar$ of Sec. III. Therefore, we obtain also $\bar{\tau}_m \propto (\bar{\omega})^{-0.6}$.

This $(\bar{\omega})^{-0.6} \approx (\bar{\omega})^{-1/2}$ dependence suggests that the special s-d exchange model of Eq. (3) may be a more exact formalism for our purpose. Data analysis is very similar. We obtain a value of the coefficient b, and consequently of the magnon conductivity $\kappa_m(T)$ at $B_{eff} = 0$. Within experimental errors, this $\kappa_m(T)$ coincides with the one obtained by the first method. The lifetimes τ_m calculated at the same frequency agree also, within ± 5%.

The 81-wt%-Ni–19-wt%-Fe data have also been analyzed with Eq. (2), and the results are given in Table I and Fig. 8. We assume[22] $g = 2.08$, $D = 4.04 \times 10^{-40}$ J m^2, and[21] $M_s = 1.09$ T. We obtain $\kappa_m \propto T^{1.5}$ for the magnon conductivity at $B_{eff} = 0$. This implies $\tau_m \propto T^{-1} \propto (\bar{\omega})^{-1}$. These temperature and frequency dependences differ from the $T^{-0.6}$ and $\omega^{-0.6}$ dependences indicated in our earlier report[6] on this work, due to improved data analysis and to a more correct expression for B_{eff}.

The reciprocal of the magnon lifetimes $\bar{\tau}_m$ of our two alloys is plotted as a function of $\bar{\omega}/2\pi$ in Fig. 9. Also shown is the reciprocal magnon lifetime $1/\tau_m = g\mu_B \mu_0 \Delta H/\hbar$ derived[23] from the ferromagnetic-resonance (FMR) linewidth ΔH, measured up to 140 GHz by Frait and MacFaden[24] in a bulk single crystal of 58-wt%-Ni–42-wt%-Fe. We also use[23] a ΔH value measured by Weber[22(b)] for spin-wave resonance (SWR) in a 81-wt%-Ni–19-wt%-Fe polycrystalline film at 57.8 GHz. The various τ_m values agree rather well. It is interesting that the

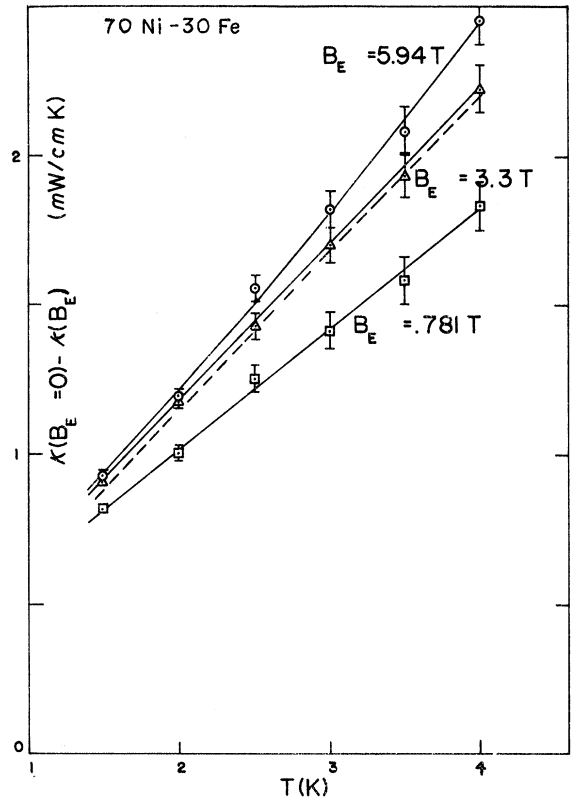

FIG. 6. Change in thermal conductivity from $B_E=0$ to a certain B_E value for 70-wt%-Ni-30-wt%-Fe. The dashed curve is the predicted change at 3.3 T as calculated from the data at 5.94 and 0.781 T.

frequency variation of the Frait-MacFaden (FMR) lifetimes is practically identical (above 50 GHz) to the variation $1/\bar{\tau}_m \propto (\bar{\omega})^{-1/2}$ of our lifetimes for the similar alloy 70Ni-30Fe. This agreement is especially remarkable because FMR and SWR magnons differ from thermal magnons in their much larger ratio of Zeeman to exchange energy and, correspondingly, their much smaller wave number q. Bagguley and Heath[25] suggested the same ω dependence for FMR lifetimes in polycrystals of other materials with low magnetic anisotropy.

Our result $\bar{\tau}_m \propto (\bar{\omega})^{-1/2} \propto T^{-1/2}$ suggests that magnon-electron scattering is the main magnon relaxation process in 70-wt%-Ni-30-wt%-Fe and that the s-d exchange is the main interaction coupling magnons and electrons. However, this frequency dependence is predicted[12,13] only if the momentum gap between spin-up and spin-down Fermi surfaces is much smaller than the magnon momentum. Existing band calculations[26(a)] for nickel show such gaps to be too large for that condition to be satisfied at 4 K, except in the vicinity of certain points of the Fermi surface. Then spin-flip scattering of electrons by magnons seems almost impossible.

If spin-orbit interaction is introduced, an anisotropic s-d exchange interaction of the pseudodipole type may exist. It induces non-spin-flip electron-magnon scattering. It is formally similar to the s-d magnetic dipole interaction treated by Abrahams[26(b)] but is of larger magnitude. It gives[20] the same $\omega^{-1/2}$ dependence as the isotropic exchange interaction, assuming the "clean" limit $\Lambda_e q \gg 1$, where Λ_e is the electron mean free path and q the magnon wave number. However, it is not affected by the momentum gap problem, since electrons make transitions between points of the same Fermi surface. Therefore it could explain our results for 70-wt%-Ni-30-wt%-Fe. It could even explain our results for 81-wt%-Ni-19-wt%-Fe, since[20] it predicts $\tau_m \propto \omega^{-1}$ in the "dirty" limit $\Lambda_e q \gg 1$.

Another way of solving the momentum gap problem involves the smearing of the gap by alloy disorder, and predicts $\tau_m \propto \omega^{-1}$. It is described in Sec. VIII. It may apply to the Ni-Fe as well as to the Ni-Cu alloys.

VIII. BREAKDOWN OF MOMENTUM GAP

We showed in Secs. VI and VII that the magnon lifetime is at least seven times shorter in the Ni-Cu sample than in the Ni-Fe samples. On the

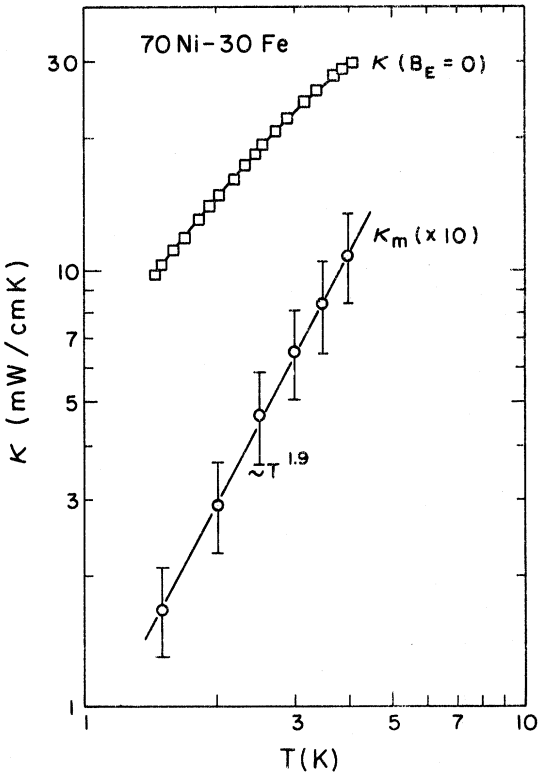

FIG. 7. Magnon thermal conductivity κ_m at $B_{eff}=0$ and the measured total thermal conductivity κ at $B_E=0$, for 70-wt%-Ni-30-wt%-Fe.

TABLE I. Experimental quantities for the two Ni-Fe alloys. Column 2 is the observed change in thermal conduction between $B_E \approx 0.75$ and 5.94 T. Column 3 is the change in electron conduction for the same fields. Column 4 is the change in magnon conduction for the same fields. Column 5 is the theoretical percent change in magnon conduction between the same fields. Columns 6 and 7 are the magnon thermal conductivity at $B_{eff}=0$ and the average lifetime of thermal magnons. Column 8 is the average frequency of thermal magnons.

T (K)	$\Delta\kappa$ (mW/cm K)	$\Delta\kappa_e$ (mW/cm K)	$\Delta\kappa_m$ (mW/cm K)	$\Delta\kappa_m/\kappa_m$ (theory)	κ_m (mW/cm K)	$\bar{\tau}_m$ (10^{-10} sec)	$\bar{f}=\bar{\omega}/2\pi$ (GHz)
			70-wt%-Ni-30-wt%-Fe				
1.5	−0.1	−0.022	−0.078	−0.466	0.167	3.0	100
2.0	−0.18	−0.03	−0.15	−0.535	0.29	2.6	133
2.5	−0.30	−0.037	−0.26	−0.556	0.47	2.4	167
3.0	−0.41	−0.044	−0.36	−0.551	0.66	2.14	200
3.5	−0.50	−0.051	−0.44	−0.531	0.84	1.86	233
4.0	−0.62	−0.059	−0.56	−0.518	1.09	1.71	266
			81-wt%-Ni-19-wt%-Fe				
1.5	−0.08	0.000	−0.08	−0.510	0.16	3.0	100
2.0	−0.12	0.000	−0.12	−0.565	0.21	1.93	133
2.5	−0.20	0.000	−0.20	−0.578	0.35	1.83	167
3.0	−0.25	0.000	−0.25	−0.560	0.45	1.49	200
3.5	−0.30	0.000	−0.30	−0.544	0.55	1.24	233
4.0	−0.37	0.000	−0.37	−0.525	0.70	1.14	266

other hand, as mentioned in these sections, there is some evidence from Peltier data[20] that magnon-electron scattering dominates over other magnon scattering mechanisms, at least in Ni-Cu. If we accept the latter evidence, then we have to explain why magnon-electron relaxation is so much faster in Ni-Cu than in Ni-Fe.

Most quantities such as the electronic density of states,[27] the exchange stiffness D, etc., are not very different in the two alloy series. But the electron relaxation times τ_e seem to differ by a factor of 5 at 4 K, as shown by the electrical resistivities: $\rho = 23.4\times10^{-8}$ Ω m for Ni-Cu vs $\rho \approx 4.3\times10^{-8}$ Ω m for the Ni-Fe samples. And the magnetizations M_s differ at least by a factor of 4, being only $M_s \approx 0.27$ T for 67-wt%-Ni-33-wt%-Cu. Both of these facts may provide an explanation for the difference in magnon lifetimes.

Starting from another deeper point of view, we recall that the simple s-d exchange model of magnon-electron scattering (see Secs. III and VII) neglects the existence of the momentum gap between spin-up and spin-down Fermi surfaces of the ferromagnet. This gap actually exists[26(a)] and is larger than the momentum of thermal magnons at 4 K. However, in the case of alloys the finite electron mean free path Λ_e leads, through the Heisenberg uncertainty principle, to a smearing $\Delta k = 1/\Lambda_e$ of the Fermi surfaces and thus to a partial disappearance of the momentum gap of pure nickel. The gap itself depends on the exchange splitting of the bands, which is proportional to the saturation magnetization M_s. Thus we can expect that the gap will be easier to bridge, and electron-magnon scattering will be stronger, in alloys with a shorter electron mean free path Λ_e, or relaxation time

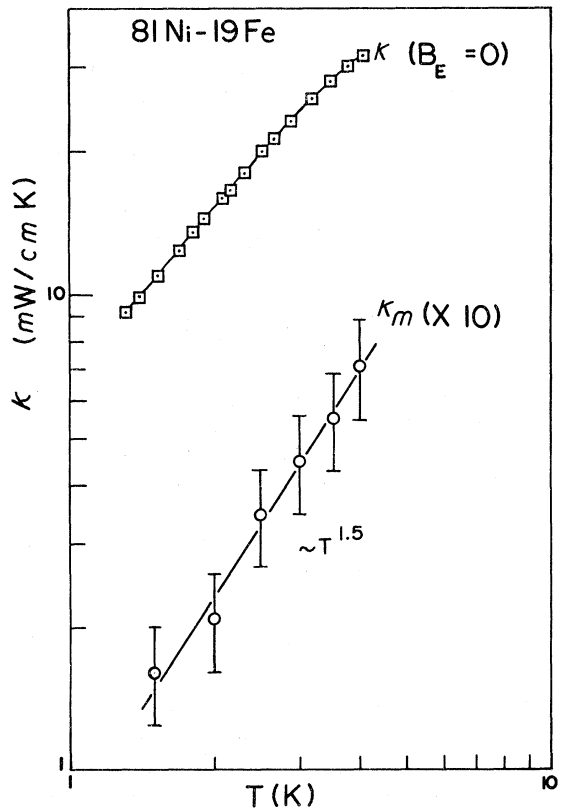

FIG. 8. Magnon thermal conductivity κ_m at $B_{eff}=0$ and the measured total thermal conductivity κ at $B_E=0$, for 81-wt%-Ni-19-wt%-Fe.

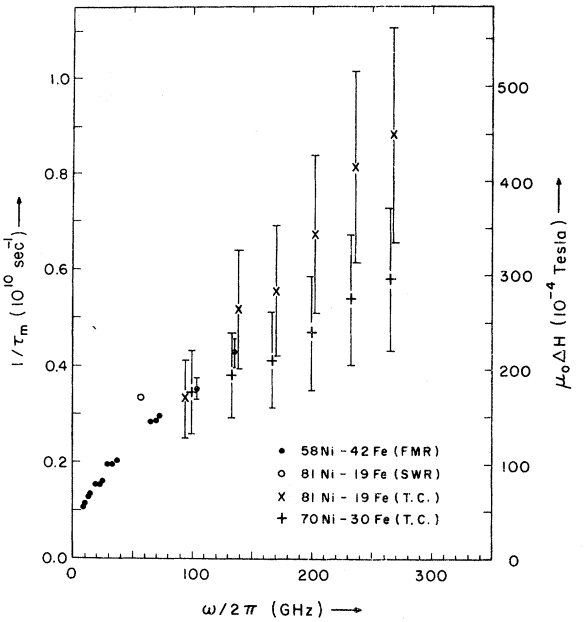

FIG. 9. Reciprocal lifetime of magnons in Fe-Ni alloys as a function of magnon frequency. SWR and FMR data refer to room temperature, while our thermal-conductivity data (TC) are for the 1.5–4.5 K range. The right-hand vertical scale gives the corresponding linewidth $\mu_0 \Delta H$, in a mks unit equivalent to the gauss.

τ_e and with a smaller magnetization M_s, in agreement with our experimental findings mentioned above.

A theory of magnon-electron scattering which takes into account this "gap-smearing" effect has been developed by Heinrich, Fraitova, and Kambersky[28] and by Turov.[29] They obtained, in mks units,

$$\frac{1}{\tau_m}=\frac{\gamma m^* k_F \omega \mu_0}{\pi M_s}\left[1+\left(\frac{\hbar}{2J_{sd}\langle s_z\rangle \tau_e}\right)^2\right]^{-1}\frac{1}{\tau_e}, \quad (8a)$$

where J_{sd} is the s-d exchange integral, k_F the Fermi wave number, m^* the electron effective mass, and $\gamma = g\mu_B/\hbar$ the spin gyromagnetic factor. This is equivalent to a Lorentzian broadening across the gap.

In the limit $|J_{sd}\langle s_z\rangle| \gg \hbar/\tau_e$, which may apply to our alloys, this reduces to

$$\frac{1}{\tau_m}=\frac{\gamma m^* k_F \mu_0}{\pi M_s}\left(\frac{\omega}{\tau_e}\right). \quad (8b)$$

Note that, according to Heinrich, Fraitova, and Kambersky,[28] τ_e in Eq. (8b) should be the electron spin relaxation time. However, it seems to us that the (much faster) momentum relaxation also contributes to the smearing of the momentum gap in the s-d exchange model [see their Eq. (12)], and we reinterpret τ_e accordingly. Thus $\tau_e \approx 10^{-13}$–10^{-14} sec in alloys.

Equation (8b) is independent of J_{sd}. Assuming $k_F \approx 10^{10}$ m^{-1}, $M_s \approx 1$ T, $\tau_e = 10^{-13} - 10^{-14}$ sec, $\omega/2\pi = 250$ GHz, it predicts $\tau_m = 10^{-10} - 10^{-11}$ sec, in rough agreement with our experimental values for Ni-Cu and Ni-Fe. According to Eq. (8b), the smaller M_s and τ_e, the easier it is to bridge the momentum gap and the shorter is τ_m. This is also consistent with our findings in comparing Ni-Cu and Ni-Fe, as discussed above. Finally, the $\tau_m \propto \omega^{-1}$ dependence predicted by Eq. (8b) agrees with our data for 81-wt%-Ni–19-wt%-Fe.

IX. CONCLUSIONS AND FINAL REMARKS

These are the first observations of magnon heat transport in transition metals. The thermal magnon lifetime is about 1.5×10^{-10} sec at 4 K in 70-wt%-Ni–30-wt%-Fe and 81-wt%-Ni–19-wt%-Fe. Fair agreement is obtained with earlier lifetime values[22(b),24] derived from spin-wave-resonance and ferromagnetic-resonance experiments above 50 GHz.

In 70-wt%-Ni–30-wt%-Fe the lifetime varies as $\omega^{-0.6}$, in approximate agreement with the simple s-d exchange theory[12,13] without momentum gap. In the alloy 81-wt%-Ni–19-wt%-Fe the lifetime varies as ω^{-1}, in better agreement with the advanced s-d exchange theory[28,29] of magnon-electron scattering, where the electron momentum gap is partially smeared away by electron relaxation effects. No magnon heat transport was detected in 67-wt%–Ni-33-wt%-Cu, implying a magnon lifetime shorter than 2×10^{-11} sec at 3.55 K. The difference between Ni-Fe and Ni-Cu lifetimes may be explained[28,29] in terms of a more complete breakdown of the electron momentum gap in Ni-Cu, resulting in stronger magnon-electron scattering. A less likely explanation involves magnon-impurity scattering, stronger in the more inhomogeneous Ni-Cu.

Use of alloys for investigation of magnon relaxation processes has several advantages: (a) Magnon heat transport is not drowned in a much larger electron contribution. (b) Electron contribution is almost field independent above ferromagnetic saturation, since $\omega_c\tau \ll 1$. (c) Small field variation of electron contribution can be subtracted precisely, using the Wiedemann-Franz law, since electron scattering is mostly elastic. (d) Phonon contribution is field independent, since electron levels undergo no Landau-Peierls quantization when $\omega_c\tau \ll 1$.

Scattering of magnons by grain boundaries should be quite negligible, since the grain size (0.1–0.5 mm) is much larger than the magnon mean free path ($\Lambda_m \approx 2\times10^{-4}$ mm). The same should be true of relaxation processes involving the surface, such as spin pinning, etc.

ACKNOWLEDGMENTS

Our thanks go to Professor S. A. Friedberg and his collaborators for advice on many aspects of the problem and for providing several computer programs used in data analysis. G. Grannemann, A. K. Majumdar, and T. O'Connell have provided assistance in some parts of the experiments. We had helpful discussions with Professor S. H. Charap, Professor A. Yelon, and Professor S. M. Bhagat.

APPENDIX

To first order in the parameter M_s/B_E, the energy of a spin wave is given by[30]

$$E(q)=Dq^2+g\mu_B(B_E+\tfrac{1}{2}M_s\sin^2\theta)\,, \tag{A1}$$

where θ is the angle between $\vec{q}$ and the magnetization $\vec{M}_s$. Generalizing the kinetic-theory expression of Sec. III for the magnon conductivity, we write

$$\kappa_m(B_E,M_s)=\iint \tau_m c(B_E,M_s)v_z^2(B_E,M_s)\frac{dN}{dq\,d\Omega}\,dq\,d\Omega\,. \tag{A2}$$

After combining Eqs. (A1) and (A2) and keeping terms up to first order in (M_s/B_E), we obtain three terms. The first is the zero-order term

$$\kappa_m^{(1)}(B_E)=\frac{1}{8\pi^3}\int \tau_m c(B_E,0)\left(\frac{2Dq}{\hbar}\right)^2 q^2dq\int\cos^2\theta\,d\Omega$$

$$=\frac{1}{6\pi^2}\int \tau_m c(B_E,0)\left(\frac{2Dq}{\hbar}\right)^2 q^2dq\,. \tag{A3}$$

The second term represents the effect of M_s on the specific heat:

$$\kappa_m^{(2)}(B_E)$$

$$=\frac{1}{8\pi^3}\int \tau_m\frac{\partial c}{\partial B_E}\left(\frac{2Dq}{\hbar}\right)^2 q^2dq\int\frac{M_s}{2}\sin^2\theta\cos^2\theta\,d\Omega$$

$$=\frac{1}{6\pi^2}\int \tau_m\frac{\partial c}{\partial B_E}\left(\frac{2Dq}{\hbar}\right)^2 q^2dq\,\frac{M_s}{5}\,.$$

Hence we can now add this to the first term:

$$\kappa_m^{(1)}(B_E)+\kappa_m^{(2)}(B_E)=\kappa_m^{(1)}(B_E+\tfrac{1}{5}M_s)\,. \tag{A4}$$

The third term in the expansion represents the effect of the magnetization on v_z:

$$\kappa_m^{(3)}(B_E)=\iint \tau_m c(B_E,0)\,[v_z^2(B_E,M_s)-v_z^2(B_E,0)]\times\frac{dN}{dq\,d\Omega}\,dq\,d\Omega\,.$$

Substituting $c(B_E,0)$ and changing variables we get from Eq. (A1), since $v_z=\hbar^{-1}\partial E/\partial q_z$,

$$\kappa_m^{(3)}(B_E)=-\frac{k_B^{7/2}T^{5/2}}{4\pi^3\hbar^2D^{1/2}}\int \tau_m\frac{(e^{x+z})(x+z)^2x^{1/2}}{(e^{x+z}-1)^2}\,dx\times\int\cos^2\theta\,\sin^2\theta\,d\Omega\frac{g\mu_BM_s}{k_BT}\,,$$

where $z=g\mu_BB_E/k_BT$. From Eq. (A3), we can show that

$$\kappa_m^{(1)}=\frac{k_B^{7/2}T^{5/2}}{3\pi^2\hbar^2D^{1/2}}\int \tau_m\frac{(e^{x+z})(x+z)^2x^{3/2}}{(e^{x+z}-1)^2}dx$$

and

$$\frac{\partial\kappa_m^{(1)}}{\partial z}=-\frac{k_B^{7/2}T^{5/2}}{2\pi^2\hbar^2D^{1/2}}\int \tau_m\frac{(e^{x+z})(x+z)^2x^{1/2}}{(e^{x+z}-1)^2}dx\,;$$

hence,

$$\kappa_m^{(3)}(B_E)=\frac{\partial\kappa_m^{(1)}}{\partial B_E}(B_E)\tfrac{4}{15}M_s\,. \tag{A5}$$

Combining Eqs. (A4) and (A5), the final result is

$$\kappa_m(B_E,M_s)=\kappa_m^{(1)}(B_E+\tfrac{7}{15}M_s)\,. \tag{A6}$$

It can be shown that the same expression holds for the s-d exchange model [see Eq. (3)].

Thus the effect of dipole-dipole interaction is, to first order in M_s/B_E, to replace the external field B_E by an effective field $B_{eff}=B_E+\frac{7}{15}M_s$.

A similar problem has been considered by Charap,[31] but the results have not been expressed in terms of an effective field.

---

*Work supported by the Army Research Office, Durham and the National Science Foundation.

†Present address: Brookhaven National Laboratories, Upton, N. Y. 11973.

[1]D. Douthett and S. A. Friedberg, Phys. Rev. 121, 1662 (1962); D. Douthett, Ph. D. thesis (Carnegie Institute of Technology, 1958) (unpublished).

[2]B. Luthi, Phys. Chem. Solids 23, 35 (1962); S. A. Friedberg and E. Harris, in *Proceedings of the Eighth International Conference on Low Temperature Physics, September*, 1972, edited by R. O. Davies (Butterworths, London, 1963), p. 302; E. Harris, Ph. D. thesis (Carnegie Institute of Technology, 1964) (unpublished); R. L. Douglass, Phys. Rev. 129, 1132 (1963).

[3]D. C. McCollum, R. L. Wild, and J. Callaway, Phys. Rev. 136, A426 (1964).

[4]J. E. Rives and D. Walton, Phys. Letters 27A, 609 (1968); J. E. Rives, G. S. Dixon, and D. Walton, J. Appl. Phys. 40, 1555 (1969); H. Weinstock, Phys. Letters 26A, 117 (1968).

[5]G. S. Nikolskii and V. V. Eremenko, Phys. Status Solidi 18, K123 (1966).

[6]W. B. Yelon and L. Berger, Phys. Rev. Letters 25, 1207 (1970). The expression for B_{eff} was written incorrectly in that publication. As a result, the temperature variation of magnon conductivity and of magnon lifetime was slightly incorrect. There was also a misprint in the definition of x.

[7]J. M. Ziman, *Principles of the Theory of Solids* (Cambridge U. P., London, 1964), p. 197.
[8]L. Berger and D. Rivier, Helv. Phys. Acta 35, 715 (1962).
[9]A. B. Pippard, Phil. Mag. 46, 1104 (1955).
[10]J. E. Zimmerman, Phys. Chem. Solids 11, 299 (1959).
[11]P. Lindenfeld and W. B. Pennebaker, Phys. Rev. 127, 1881 (1962).
[12]E. A. Turov, Izv. Akad. Nauk SSSR, Ser. Fiz. 19, 462(1955)[Bull. Acad. Sci. USSR, Phys. Ser. 19, 414 (1955)]; A. H. Mitchell, Phys. Rev. 105, 1439 (1957).
[13]S. V. Vonsovskii and Yu. A. Izyumov, Phys. Metals Metallogr. (USSR) 10, 1 (1960).
[14]J. B. Sousa, Cryogenics 8, 105 (1968).
[15]J. R. Clement and E. H. Quinnell, Rev. Sci. Instr. 23, 213 (1952).
[16]C. J. Adkins, J. Sci. Instr. 38, 305 (1961).
[17]H. Nose, J. Phys. Soc. Japan 16, 342 (1961); 16, 2475 (1961); E. I. Kondorskii, V. E. Rode, and U. Gofman, Zh. Eksperim. i Teor. Fiz. 35, 549 (1958) [Sov. Phys. JETP 8, 380 (1959)].
[18]J. W. Cable, E. O. Wollan, and H. R. Child, Phys. Rev. Letters 22, 1256 (1969).
[19]S. C. Moss, Phys. Rev. Letters 23, 381 (1969).
[20]G. N. Grannemann and L. Berger (unpublished).
[21]R. M. Bozorth, *Ferromagnetism* (Van Nostrand, New York, 1951).
[22](a) G. I. Rusov, V. G. Pyn'ko, and A. A. Nedelko, Izv. Akad. Nauk SSSR, Ser. Fiz. 31, 443 (1967) [Bull. Acad. Sci. USSR, Phys. Ser. 31, 460 (1967)]. (b) M. H. Seavey, Phys. Rev. 170, 560 (1968); R. Weber, *ibid.* 169, 451 (1968).
[23]This ΔH is the difference of the fields where the imaginary part $\mathrm{Im}\mu_{eq}$ of the equivalent permeability is half of its maximum value. If $\mathrm{Im}\mu_{eq}$ is Lorentzian, then this ΔH is 0.8 of the linewidths quoted by Frait and MacFaden (Ref. 24).
[24]Z. Frait and H. MacFaden, Phys. Rev. 139, A1173 (1965).
[25]D. M. S. Bagguley and M. Heath, Proc. Phys. Soc. (London) 90, 1029 (1967); 90, 1047 (1967).
[26](a) J. W. D. Connolly, Phys. Rev. 159, 415 (1967). See his Figs. 6 and 7. The momentum gap of the 4*s* band is smallest. (b) E. Abrahams, Phys. Rev. 98, 387 (1955). See his Sec. IV.
[27]R. Ehrat and D. Rivier, Helv. Phys. Acta 33, 954 (1960). See their Fig. 2.
[28]B. Heinrich, D. Fraitova, and V. Kambersky, Phys. Status Solidi 23, 501 (1967); Phys. Letters 23, 26 (1966).
[29]E. A. Turov, in *Ferromagnetic Resonance*, edited by S. V. Vonsovskii (Israel program for scientific translations, Jerusalem, 1964), p. 132.
[30]T. Holstein and H. Primakoff, Phys. Rev. 58, 1098 (1940).
[31]S. H. Charap, Phys. Rev. Letters 13, 237 (1964).

PHYSICAL REVIEW B VOLUME 6, NUMBER 5 1 SEPTEMBER 1972

Paramagnetic Susceptibilities of Metallic Samarium Compounds

A. M. Stewart
Istituto di Fisica, Università di Genova, 5 Viale Benedetto XV, Genova CAP 16132, Italy and Department of Electrical Engineering and Department of Physics, Imperial College, London S.W.7, England*
(Received 8 February 1972)

It is shown that the influence of conduction-electron polarization effects upon the susceptibilities of metals containing the tripositive samarium ion is very much greater than upon metals containing normal rare earths. A theory of the susceptibility of metallic samarium materials is developed which takes account of these polarization effects and of interionic Heisenberg exchange couplings, the admixture of the $J=\frac{7}{2}$ state into the $J=\frac{5}{2}$ ground state, which is assumed to be the only one to be thermally populated, but which, however, does not take account of crystal-field splittings. The susceptibility is found to be of the unexpectedly simple form $\chi(T)=\chi_0+D/(T-\theta)$, in which the only dependence on temperature T is that explicitly shown. This expression is found to fit the published data for the susceptibility of dhcp samarium to an accuracy of 1% in the temperature region 110–230 °K, and the parameters extracted from the fit are found to be in excellent agreement with those obtained for the other light rare-earth metals. An expression is also derived for the susceptibilities of metals containing normal rare earths, which takes account of both conduction-electron polarization and crystal field effects.

I. INTRODUCTION

The purpose of this paper is to direct attention to the effects of conduction-electron spin polarization upon the paramagnetic susceptibilities of metallic rare-earth compounds, in particular those containing samarium. Although for "normal" rare-earth ions (that is, those whose properties may be adequately described by taking account only of the lowest angular momentum level of quantum number J) the effects of conduction-electron spin polarization upon the paramagnetic susceptibility are rather small—of the order of a few percent—they are nonetheless important to measure because